

DRY COUPLING, LAMBDA, AND GEOMETRICAL ACOUSTIC TRANSDUCERS - THREE JEWELS FOR ULTRASONIC NDC

M. C. Bhardwaj
Ultran Laboratories, Inc.
State College, PA

A PUBLICATION OF ULTRAN LABORATORIES, INC., Series on NDC, EPN-101b - July 1987

ultran

redefining
the limits of
ultrasound

ultran laboratories, inc.
139R north gill street
state college, pa 16801 usa
814.238.9083 *phone*
82.0978 *telex*
814.234.3367 *fax*

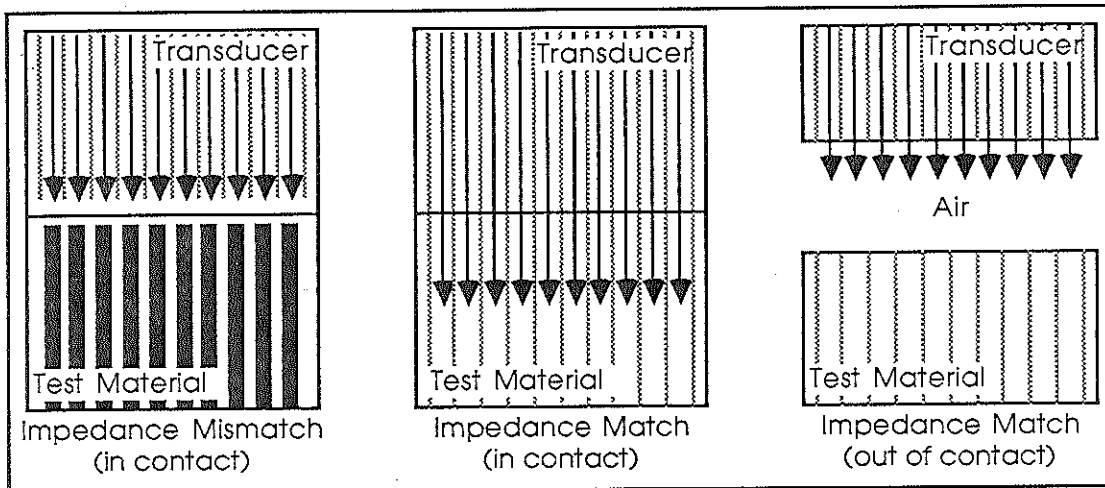


Fig. 1. A graphical representation of acoustic impedance match and mis-match conditions when ultrasound travels from an active transducer into media of varying acoustic impedances.

In order to alleviate the problem of impedance matching as well as to make a "good" contact of the transducer to the test material surface without sacrificing the amount of ultrasonic energy transfer into the material, a new interfacial material had to be developed and implanted on the piezoelectric element. After several years of "trial-and-error," in 1982 we developed a polymer in our laboratory that met all our criteria for DIRECT and DRY COUPLING CONTACT. This material, known as the "solid compliant transitional layer," acts as a "built-in" couplant inside the transducer device. Fig. 2 graphically illustrates the mechanism of a dry coupling transducer concept. The pliable transitional layer is relatively acoustically transparent over a wide range of frequencies, and resilient enough to make good contact with the test material surface.

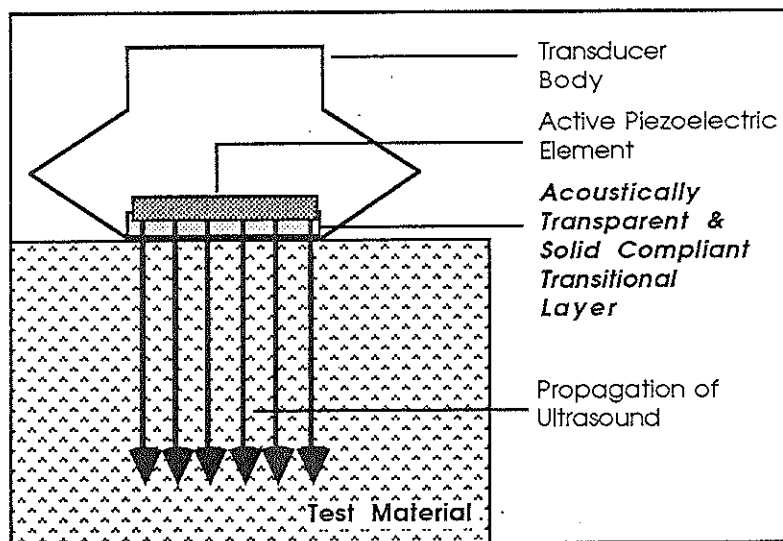


Fig. 2. A graphical explanation of the principle of Dry Coupling ultrasonics. Transducers based upon this design have been optimized for 0° incidence longitudinal and shear wave propagation from <100KHz to >25MHz.

Brunk (1985, 86, & 87)^{2,3,4} has favorably compared dry coupling transducers and their conventional wet-coupled counterparts in several thickness measurement applications. In several instances he has shown that dry coupling technique is more dependable.

Following the success in longitudinal wave dry coupling transducers, we have successfully applied this technique even for the propagation of 0° shear waves in solid media. Longitudinal and shear wave transducers for straight and delayed contact have been perfected in frequencies ranging from <100KHz to >25MHz. Here we present performance and applications of dry coupling ultrasonic technique.

Comparison of ultrasonic energy transfer by dry and wet coupling techniques

Fig. 3 shows dual oscilloscope traces of rf A-scans obtained by the direct reflection method from 10MHz wet and dry coupled ultrasonic transducers on a 99.3% dense and impervious Al_2O_3 sample. Observe the similarity in the strength of reflected signals in both cases, proving that ultrasonic energy transfer by dry coupling is adequate for making accurate time-of-flight measurements. For example, the measured times-of-flight in both techniques on this sample is exactly the same, i.e., $1.88\mu s$.

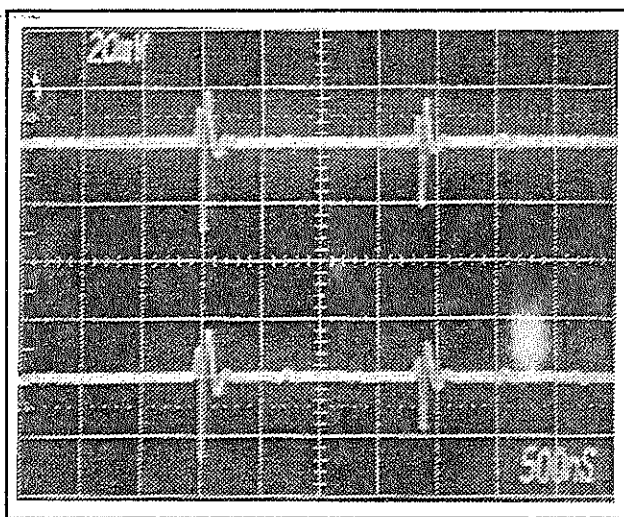


Fig. 3. Realtime rf A-scan traces generated by using WET (top) and DRY (bottom) coupling ultrasonic transducers on a 99.3% dense and IMPERVIOUS Al_2O_3 sample 10.3mm thick. In both cases 10MHz and 6mm active area diameter transducers were used to demonstrate "excellent" comparison between wet and dry coupling techniques while examining impervious materials.

Observe the similarity in the amplitudes of signals representing top (left hand signal) and bottom (right hand signal) surfaces of the test material.

Unreliability of wet coupling for porous material analysis

CASE I. Instantaneous absorption of liquid. Fig. 4 is dual oscilloscope traces of rf A-scans obtained by the direct reflection technique from a 10MHz wet coupled transducer on a 64.8% dense Al_2O_3 sample characterized by open porosity. The top trace was obtained as soon as the liquid couplant (in this case glycerene) was applied to the sample surface. The bottom trace was taken two to three seconds after the application of liquid couplant. The effect of couplant on ultrasonic observations is dramatic. As soon as it is poured on this material, the couplant is instantaneously absorbed by the material porosity, making a reliable observation virtually impossible and frustrating. On the other hand, application of a dry coupling transducer on this

material at different intervals of time shows neither any variations in ultrasonic observations nor in the strength of ultrasonic signals, Fig. 5.

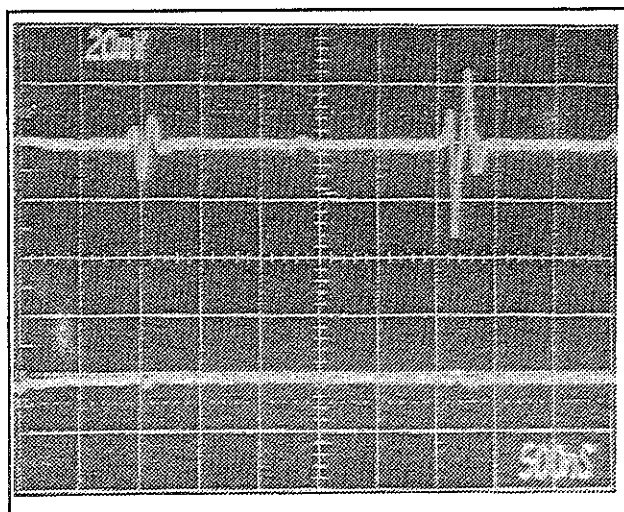


Fig. 4. RF A-scans produced by using WET coupling technique on a 64.8% dense POROUS sample of Al_2O_3 .

Top trace was photographed "as soon as" the couplant (glycerine) drop was applied on the sample surface, while the bottom trace was taken "a couple of seconds" after the couplant application. Comparison of these observations clearly prove the unreliability of wet coupling for porous media.

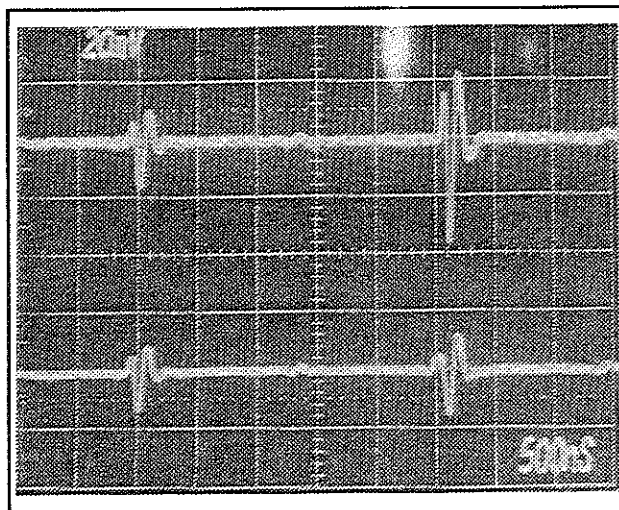


Fig. 5. Same conditions as in Fig. 4, except, here DRY coupling technique was applied on POROUS material.

The time difference between photographing top and bottom traces is several hours. These observations clearly prove the reliability of dry coupling for the investigation of porous materials.

CASE II. Erroneous conclusions by wet coupling. A direct bonded fused silica refractory sample of 20% open porosity and approximately $50\mu\text{m}$ particle size was analyzed in its dry and wet conditions by a dry coupling transducer in order to observe the effects of partial saturation (of this sample) with water. In its "true" dry state, the round-trip time-of-flight of ultrasound propagation is $8.9\mu\text{s}$. The same sample was submerged in water for approximately 15 minutes, and subsequently subjected to a similar ultrasonic examination by the same dry coupling transducer. The round-trip time-of-flight measured for this condition is $8.6\mu\text{s}$. The thickness of the sample investigated is 19mm. Therefore, if the velocities were determined from this experiment, the following conclusions would have been drawn:

1. Measured velocity by dry coupling, representative of the TRUE state of material is 4270m/s.
2. Measured velocity by wet coupling, representative of the ALTERED state of material is 4420m/s. Since velocity of a material is directly related to its micro-structure and elastic properties, any conclusions drawn from wet coupling (particularly on relatively porous materials) would be wrong. In this case, pores that were once filled with air in the material's true state are actually now filled with water, producing the higher velocity with wet coupling. The velocity of water (1480m/s) is higher than that of air (343m/s), thus water-filled material gives a higher velocity. In fact, the examination of porous materials by the wet coupling technique actually gives information about "something other than" the real material.

We have successfully used dry coupling technique for the measurement of longitudinal and shear wave velocities and other characteristics of green and sintered as cast, as fired, and machined ceramics and powder metals, and other materials. However, if the surfaces of test materials are granulated, corrugated, or otherwise very rough, then dry coupling technique may not be applicable. There are other methods for the ultrasonic characterization of such materials; their description here is beyond the scope of this paper. Table I provides acoustic and elastic properties of selected materials determined by dry coupling technique.

Table I. Acoustic and elastic properties characterization of selected materials derived from dry coupling ultrasonic technique.

ULTRASONIC PARAMETERS & PROPERTIES	SiC ^a DENSE	SiO ₂ ^b SLIP-CAST REFRACTORY	Float ^c GLASS	BeO ^d DENSE	AZS ^e REFRACTORY
Longitudinal Velocity (m/s)	11,820	4,140	5,816	12,190	6,880
Shear Velocity (m/s)	7,500	2,740	3,460	7,360	4,210
Acoustic Impedance (g/cm ² x 10 ⁵)	37.8	7.4	14.6	36.6	25.4
Poisson's Ratio (σ)	0.17	0.11	0.23	0.21	0.20
Young's Modulus (GPa)	397	30	72	396	158
Shear Modulus (GPa)	180	13	30	162	65
Sample Size (mm)	19.5	19	6	1.07	52.6
Frequency Longitudinal Wave (MHz)	10	1	10	20	1
Frequency Shear Wave (MHz)	10	1	10	10	1

^aSOHIO Engineered Materials, ^bThermo Materials Corp., ^cPPG Industries Inc., ^dBrush Wellman, Inc., ^eMonofrax Division, SOHIO Engineered Materials.

Styles of DRY COUPLING transducers

Dry coupling devices for both longitudinal and shear wave propagation have been satisfactorily developed in direct and delayed contact styles. Even novel surface wave devices have been generated by utilizing the dry coupling mechanism!

Dry coupling ultrasonic technique is recommended when:

1. Use of liquid couplants is a nuisance.
2. Liquid couplants are expected to damage and/or alter the characteristics of the test materials.
3. Accurate measurements of porous materials is desired.

4. *Complex-shaped components are involved.*

2. LAMBDA (UNIPOLAR IMPULSE) TRANSDUCERS

One of the most critical requirement in NDC is the ability of ultrasonic wave to provide the "utmost" in the resolution of two closely lying planes as well as in detecting the defects/reflectors, lying "close" to the test material surface. Bragg's law of diffraction provides sufficient conditions for the resolution of two planes, separated by a distance, d , i.e.,

$$n\lambda = 2d \sin \theta \quad (1)$$

where, n is the order of reflection, λ , the wavelength of the interrogating beam, and θ the angle of diffraction. This angle is 90° at normal incidence of the beam (common condition in ultrasonic testing by direct reflection technique). When the order of reflection is 1, then,

$$\lambda = 2d, \text{ or} \quad (2)$$

$$d_{\min} = \lambda/2, \quad (3)$$

d_{\min} being the minimum resolvable distance in a given medium of ultrasound propagation. In order to achieve this condition the width of the pulse, i.e., the time domain of the interrogating wave must correspond to $\lambda/2$. In time domain measurements, it is desirable to have an ultrasonic wave that would "occupy" time corresponding to half the wavelength of the transducer impulse. For example, the pulse width of one wavelength of a 10MHz wave = 100ns, and that of its half wavelength counterpart, it is = 50ns.

If we were to examine dense BeO substrate, a 100ns pulse ultrasound (by direct reflection technique) would resolve to a maximum of 0.6mm, while a 50ns would increase resolution to 0.3mm, (assuming the velocity of ultrasound for BeO to be 12,000m/s). The advantage of a short pulse width is obvious. However, due to the strong dependency of resolution on the wavelength, high resolution in higher velocity materials is generally more difficult to achieve as this demands reduction of the transducer or ultrasonic system's pulse width. Reduction of transducer pulse width can be accomplished by the following mechanisms:

1. *Increasing the incident frequency.*
2. *Minimizing the transducer resonance.*
3. *Simultaneously increasing the frequency and minimizing the resonance.*
4. *Through complicated electronic systems, or mathematical treatment of an otherwise broad pulse.*

While the transducer frequency must be increased to some level in order to achieve the desired resolution, it should be noted that increased frequency does not necessarily guarantee reduced pulse width. High frequency transducers (with the exception of PVDF-based devices), generally 20MHz and above, are usually characterized by 2 to 6 wavelength pulse widths, and therefore may not necessarily suit a specific resolution goal. Furthermore, those familiar with VHF ultrasound know that indiscriminate increase of transducer frequency causes more problems rather than achieving the desired resolution objectives. These problems are related to excessive attenuation of VHF, fragility of transducers and systems limitations, Bhardwaj (1986)⁵.

However, it is possible to control the resonance of transducers up to certain higher frequencies in such a manner that the pulse width corresponds to half or one wavelength of certain frequency. Nearly 10 years ago we conceived a transducer design that appeared to show the promise of

greatly reduced pulse width. Accordingly, a transducer was first made in 1979 in our laboratory with nominal 1MHz frequency. Acoustic analysis of this device showed a dramatically reduced pulse width, corresponding to half the wavelength of 1MHz! Since then, LAMBDA transducers varying in frequency from <500KHz to nearly 30MHz have been perfected in our laboratory.

The following observations prove that λ -series transducers are typically characterized by 0.5 to 1.0 wavelength pulse width and bandwidths ranging from 100 to 300% of their center frequencies. With the development of such devices, it is possible to achieve near theoretical resolution and "very" near surface defect characterization. Further details on λ transducers are given elsewhere, Ultrason (1982)⁶.

Acoustical comparison of conventional "broadband" and λ transducers

CASE I. Planar or unfocused transducers. Fig. 6 shows the combined realtime and frequency domain analysis of a conventional 10MHz, 6mm active area diameter, "broad bandwidth" transducer. This data was obtained by exciting the transducer with a commercial "broad bandwidth" pulser-receiver. The reflecting target is an optically flat, polished and clear fused quartz surface in water. The center frequency of this transducer is 10.0MHz, bandwidth 6.0MHz or 60% of the center frequency, and pulse width 220ns.

Now compare a similar response, Fig. 7, from a λ transducer of nominal 10MHz frequency and 6mm active area diameter. Its measured center frequency is 12.0MHz, bandwidth at -6dB is 14.0 or 116% of the center frequency, and pulse width 85ns.

CASE II. Focused transducers. Fig. 8 shows the acoustic analysis of a conventional "broad bandwidth" transducer of a nominal 10MHz frequency, 6mm active area diameter, and 19mm point focus in water. The distance from the transducer to the reflecting surface corresponds to 19mm, the focal length of the transducer. The measured center frequency of this device is 9.5MHz, bandwidth 9.0MHz or 95% of the center frequency, and pulse width 100ns. For most practical purposes, this is an excellent device; however, an equivalent λ transducer is even superior!

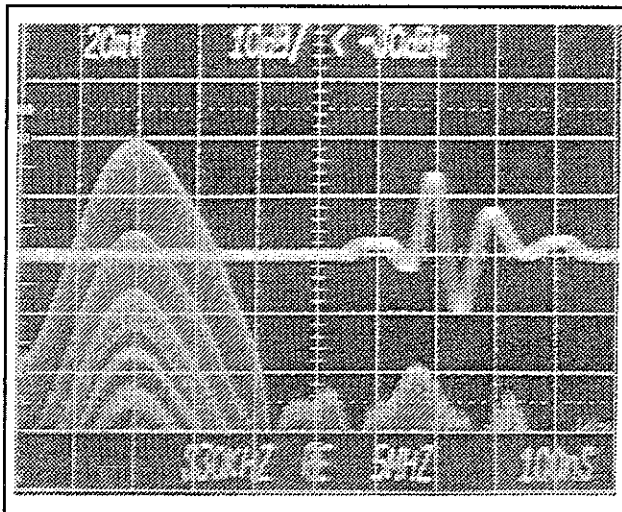


Fig. 6. Time and frequency domain analysis of a conventional "broadband" transducer - nominally 10MHz and 6mm active area diameter - PLANAR.
bcf (bandwidth center frequency) = 10MHz
Bandwidth at -6dB = 6MHz or 60%
Pulse width = 220ns.

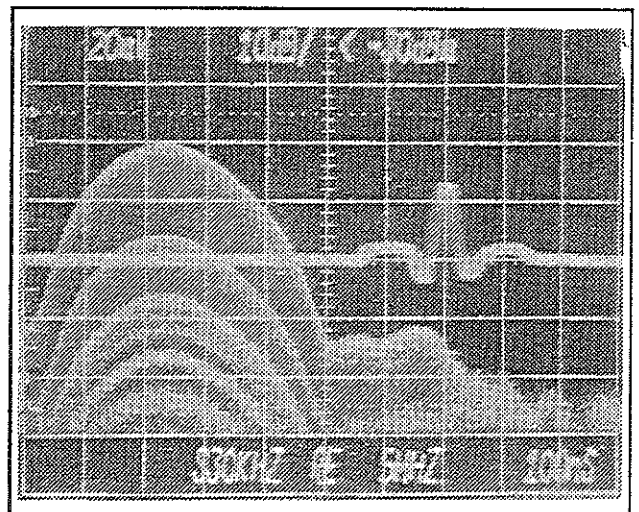


Fig. 7. Same as Fig. 6, except for a λ transducer.
bcf = 11.5MHz
Bandwidth = 14MHz or 122%
Pulse width = 85ns.

Fig. 9 shows the acoustic characteristics of a λ transducer of nominal 10MHz frequency, 6mm active area diameter, and 19mm point focus in water. The measured center frequency of this device - although somewhat meaningless due to a "flat" frequency response - is 19.5MHz, bandwidth at -6dB is from 3 to 36MHz (33MHz or 170% of the center frequency 19.5MHz), and the pulse width is 50ns. Compare these characteristics with the conventional comparable transducer in Fig. 8.

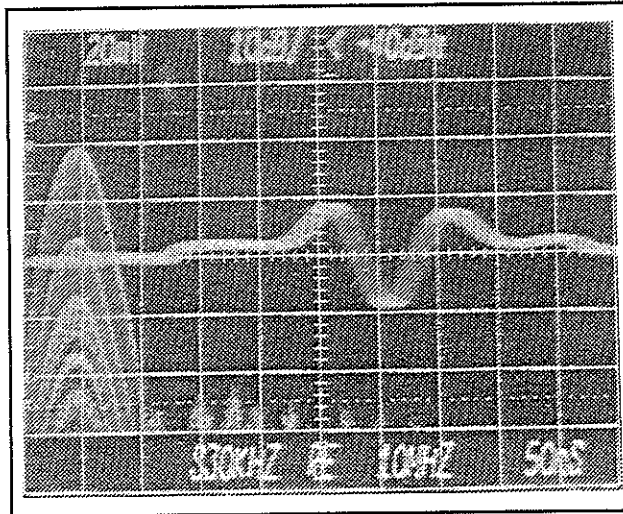


Fig. 8. Time and frequency domain analysis of a conventional "broadband" transducer - nominally 10MHz and 6mm active area diameter, 19mm FOCUSED.
bcf = 9.5MHz
Bandwidth at -6dB = 9MHz or 95%
Pulse width = 100ns.

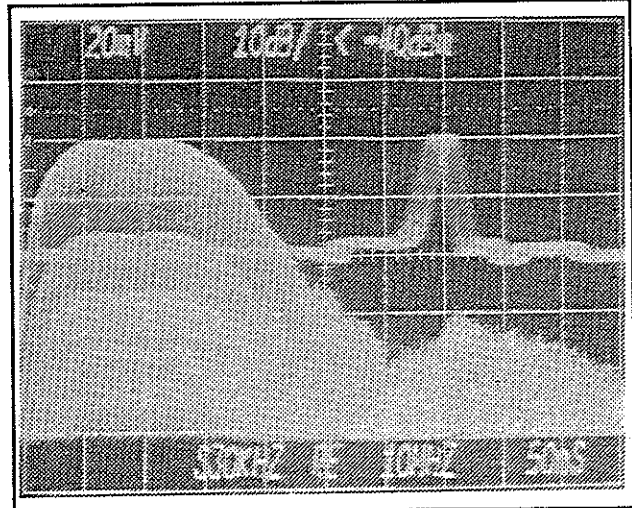


Fig. 9. Same as Fig. 6, except for a λ transducer.
bcf = 19MHz - practically "flat response!"
Bandwidth = 33MHz or 175%
Pulse width = 50ns!

Table II shows a one-to-one comparison of the acoustic data of planar and focused 10MHz conventional "broad bandwidth" and a λ transducers.

Table II. Acoustic comparison of conventional "broad bandwidth" and λ transducers. For further details, see Figures 6, 7, 8, and 9.

ACOUSTICAL AND PHYSICAL PARAMETERS	TRANSDUCERS			
	CONVENTIONAL		LAMBDA	
	PLANAR	FOCUSED	PLANAR	FOCUSED
Active Element (mm)	6.0	6.0	6.0	6.0
Center Frequency (MHz)	10.0	9.5	12.0	flat (19.5)
Bandwidth at -6dB (MHz)	6.0	9.0	14.0	33.0
Bandwidth (%Cf)	60	95	116	170
Pulse Width (ns)	220	100	85	50
Focal Length	---	19	---	19

Performance comparison of conventional "broadband" and λ transducers

CASE I. Time/distance/thickness resolution: A 1.07mm thick sample of dense BeO substrate was investigated by using planar beam conventional and λ transducers with direct reflection technique. Results of this experiment are shown in Fig. 10. The top trace corresponds to a

conventional 10MHz transducer; the bottom one to a 10MHz λ transducer. Observe "near complete submergence" of the first reflection from the bottom surface of BeO in the pulse width (the transducer-top material surface interface). It can be observed that this transducer "poorly" resolves a 1.07mm of dense BeO, and yet multiple reflections from the thickness of this material are distinguishable.

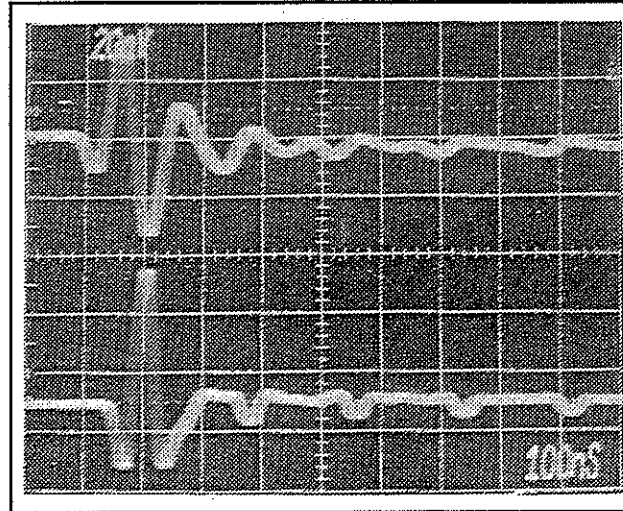


Fig. 10. Comparison of resolution capabilities of conventional "broadband" and λ transducers, each 10MHz and 6mm active area diameter.

TOP TRACE: Results from conventional transducer - poorly resolving top and bottom surfaces of a 1.07mm BeO plate.

BOTTOM TRACE: Results from a λ transducer - complete resolution of top and bottom surfaces of 1.07mm BeO plate.

The bottom trace in Fig. 10 shows the observations from a 10MHz λ transducer. It is obvious that the bottom surface of BeO is clearly resolved from the top material surface. In fact, we predict that this particular device would resolve down to 0.5mm in dense BeO. The wavelength of ultrasound in BeO at 10MHz is 1.2mm, thus allowing maximum $\lambda/2$ resolution of 0.6mm. By using the direct reflection technique actually measured time of flight is twice the thickness, thus the resolution capability is increased by another 100%! Therefore, if the transducer pulse width is truly $\lambda/2$, the actual resolution of two closely lying surfaces will be $\lambda/4$! Such observations can be noted with focused λ transducers.

CASE II. Shallow sub-surface defect detection. In order to exhibit performance comparison of the performance between conventional and λ transducers, a 1mm simulated defect, located at 0.4mm in aluminum was analyzed. In order to resolve this defect, 19mm focused and 10MHz transducers of conventional and λ designs were used. Fig. 11 shows the results of this experiment. The top surface realtime trace was obtained by the conventional focused transducer. The first reflection from the simulated defect is barely resolved by this transducer as it is "nearly lost" within the pulse width of the transducer. The multiple reflections from this defect are so closely spaced that the identification and interpretation of this defect are quite difficult.

The bottom trace in Fig. 11 was generated by using a λ transducer, 10MHz, 6mm diameter and 19mm point focused, on the same specimen as used with the conventional transducer. Because the spacing between the interface (top material surface) and first reflection from the hole is considerably large, we estimate that this particular λ transducer would resolve even if this defect was located at approximately 0.2mm in aluminum!

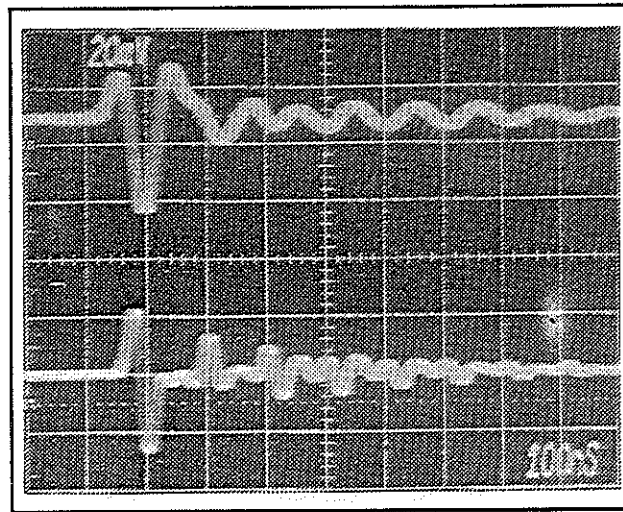


Fig. 11. Comparison of sub-surface defect detection by conventional and λ focused transducer. Target is a 1mm diameter flat bottom hole in aluminum located at ~ 0.4 mm from the test surface.

TOP TRACE: Conventional transducer - poor to no resolution of the target from test surface.

BOTTOM TRACE: λ transducer - complete resolution of the target from test surface. In fact, the same device in aluminum is capable of providing resolution better than 0.2mm.

Wideband ultrasonic spectroscopy with λ -series transducers

With the exceptional bandwidth and "purity of concentration of a large number of frequencies" in a single λ transducer, it is relatively easy to conduct ultrasonic spectroscopy over a wide frequency range. λ transducers represent a near "perfect source of white ultrasound," thus highly suitable for the analysis of frequency-dependence of ultrasound attenuation. Detailed description of ultrasonic spectroscopy is beyond the scope of this paper, and will be treated separately.

Styles of LAMBDA transducers

Lambda transducers have been successfully developed for their uses as direct high impedance contact, delay line contact, and dry coupling contact types, besides the immersion styles, as shown here.

Lambda transducers are recommended for the following materials characterization applications:

1. Extremely high resolution.
2. Phase transformation studies.
3. Ultrasonic microscopy.
4. In those studies where collimation of ultrasound is desired.
5. When accurate transit times need to be measured.
6. Minute and shallow surface defect detection.
7. Surface-breaking defects detection.

8. *Frequency dependence of ultrasonic attenuation/absorption.*
9. *In those studies where near field effects must be minimized, and*
10. *When accurate thickness/thinness measurements are required.*

3. GEOMETRICAL-ACOUSTICS TRANSDUCERS

Detection of surface and very shallow sub-surface defects in materials is highly desired, particularly in advanced ceramics and composites that are used for structural applications in automotive, aircraft/aerospace, nuclear, and defense industries; electronic materials such as ceramic substrates, capacitors, resistors, etc.; and biological components as replacement materials for bones and teeth. Ultrasonic analysis of critical surface characterization requires special attention.

In the previous section we showed the sensitivity of λ transducers for the detection of sub-surface defects. With further modifications, these devices can be used to detect minute surface defects. However, for even more confident and reliable detection and quantification of both surface and very shallow subsurface defects, a transducer must be designed in such a manner that it exhibits "perfection" in acoustics and geometry simultaneously.

Geometrical acoustics transducers - exhibiting near perfect geometrical-acoustics were first made in our laboratory in 1982 in frequencies <5MHz. However, in 1986 these devices were fabricated in frequencies ranging from 15 to >75MHz. Gilmore, et. al., (1986)⁷, also reported the use of similar transducer principles and concepts in the development of their acoustic microscope at the R & D laboratory of the General Electric Company.

Geometrical-Acoustics, or GA transducers are characterized simultaneously by controlled numerical apertures and "crisp" acoustics. In the following sections we offer a brief introduction to the geometry and acoustics of this transducer design.

Geometry of GA transducers and its relevance in materials characterization

Analysis of surface wave (Rayleigh wave) propagation can provide significant information about test material surfaces, including the detection of surface defects. In order to generate surface waves in a material, the entry angle of ultrasound with respect to the surface of the material should be well within the proximity of the second critical angle of incidence in the material:

$$\psi^* = \sin^{-1} (V_l/V_t) \quad (4)$$

where ψ^* is the second critical angle of incidence, V_l the velocity of longitudinal wave in the incident medium, and V_t is the velocity of transverse wave in the medium of refraction, Bhardwaj (1986)⁵. At this angle there is total reflection of the refracted transverse wave, thus propagating only the surface waves in the material. For example, ψ^* in dense BeO substrate is 11.5° , assuming the longitudinal wave velocity of the incident or carrier medium water being 1480m/s, and the velocity of transverse wave in BeO being 7360m/s. The depth of penetration at the second critical angle is assumed as one wavelength of the surface wave in the refracting medium, Bergmann approximation (1954)⁸.

If the angle of incidence is equal to or "slightly" more than the second critical angle, then the propagation of the longitudinal wave in the refracting medium is eliminated, thus facilitating the generation of only surface waves in the material. In experimental terms, exactly how the angle of incidence is related to the depth of the surface wave penetration is not clearly defined. Treatment of this subject is beyond the scope of this paper.

In the GA transducers, the angle of incidence is controlled by the numerical aperture (na) of the transducer. Analogous to propagation of light in an optical lens, na for GA transducers can be described as,

$$na = 2\mu \sin \alpha \text{ (for an optical lens) , and } (5)$$

$$na = 2 \sin \alpha \text{ (for a GA-series transducer) } (6)$$

where, μ is the index of refraction of an optical lens, α is half the angular aperture, or half the cone angle of the converging light or ultrasound from their respective lenses. If a geometrical acoustics design is based upon super-imposing an acoustic lens on a planar piezoelectric element, then the "acoustic index of refraction" of the lens material will have to be considered. For brevity sake, we shall simply conclude that "super-imposed-lens" focused ultrasonic transducers mathematically cannot achieve the numerical apertures corresponding to those of the GA transducers. GA transducers are characterized by "true" focusing mechanism, thus they are also free from "acoustic aberrations," present in "super-imposed-lens" designs.

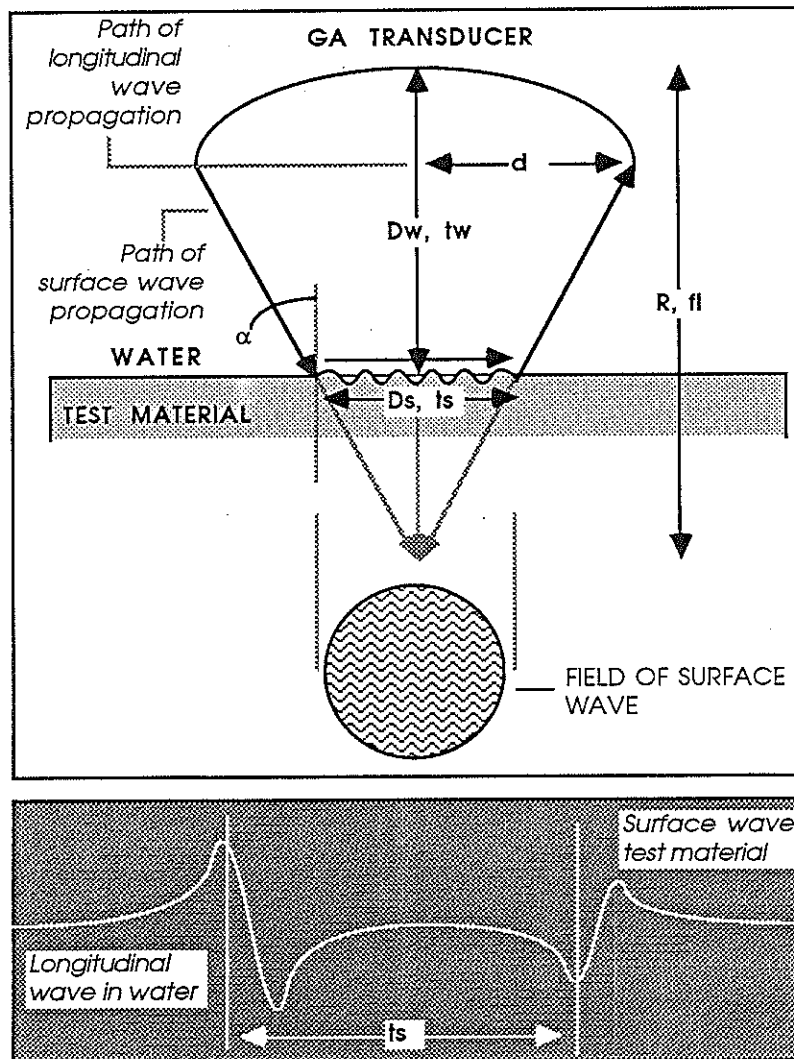


Fig. 12. Mechanism of surface wave generation by a GA transducer and explanation of wave propagation in carrier medium water into a test material. Bottom portion of this figure shows an idealized time domain representing the indications of longitudinal wave in water and surface wave in the test material.

Mechanism of surface wave generation: Fig. 12 shows the path of ultrasound propagation from a "spherically focused" GA transducer through carrier medium, water, into a solid material, generating surface waves in it. Explanation of various terms are:

d = radius of the active transducer (not half of the arc)

D_w = center line distance from transducer to material surface in water

t_w = time-of-flight of longitudinal wave in water, corresponding to D_w

D_s = distance traveled by surface waves, corresponding to the diameter of the "sliced" cone of ultrasound emanating from the transducer.

t_s = time-of-flight of surface wave, corresponding to D_s

R = radius of curvature of the active transducer, also its focal length, f_l .

α = incident or entry angle of ultrasound into the material, also half the "angular aperture" of the transducer. For surface wave generation into the test medium, this angle must be equal to or $>$ the second critical angle, ψ , in the test material.

Important relationships derived from Fig. 12 are:

$$na = 2\sin \alpha = R(d)/d = 2d/R (F.L.) \quad (7)$$

$$\text{Relative aperture, } ra = f_l/2d \quad (8)$$

$$t_w, (\text{round trip time of flight}) = 2D_w/V_w \quad (9)$$

$$t_s = 2(R - D_w) \tan \alpha / V_s \quad (10)$$

$$D_s = 2((R - D_w) \tan \alpha) \quad (11)$$

In these relationships, V_w , and V_s , are respectively, longitudinal velocity in water and surface wave velocity in test material. Surface wave time-of-flight, t_s , can be directly measured from the realtime rf trace, bottom portion of Fig. 12. D_s , besides its calculation from eq. 11, can also be estimated from the known geometry of GA transducer and its distance D_w in water. These measurements can be used to determine the surface wave velocities.

Acoustics of GA transducers

Figures 13 and 14, respectively show the realtime rf trace and Fourier spectrum of a GA-series transducer characterized by nominal 25MHz frequency, 6mm active area diameter, and numerical aperture of 1. From these observations, the measured center frequency of this transducer is 28MHz, bandwidth at -6dB is 110% of the center frequency (or ranging from 12MHz to 44MHz), and pulse width at the focal point is 35ns. This data clearly indicates the near "perfect" acoustics of this device.

Applications of GA transducers

Generation of surface waves: In order to exhibit the formation of surface waves in a material, a GA transducer with nominal 25MHz frequency, 6mm active area diameter, and 1.0na was separated in water from a glass plate by 3.5mm. This distance corresponds to 58% of the focal length of this transducer. Fig. 15 shows the real time rf trace of this condition. The signal at extreme left is the initial pulse; the one on the left hand side of the central (highlighted) region is the appearance of the longitudinal wave - directly reflected from the central point of the transducer

from the surface of glass plate. The right hand side of the highlighted region is the appearance of the surface wave from the glass plate. Fig. 16 is the amplified version of the central highlighted region of Fig. 15.

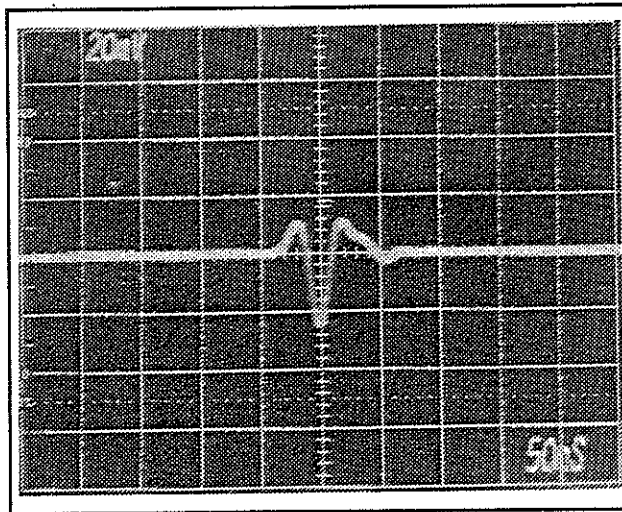


Fig. 13. Time domain analysis of a GA transducer, nominally 25MHz, active area diameter 6mm, and n_a , 1. Measured pulse width = 35ns

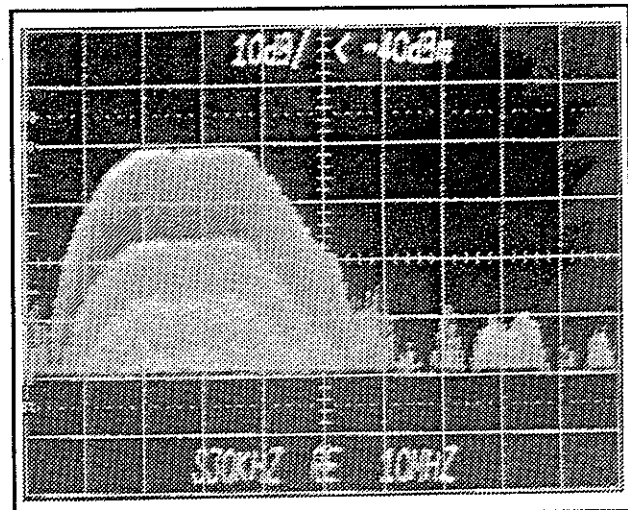


Fig. 14. Frequency domain of trace in Fig. 12 Bcf = 28MHz Bandwidth = 110% or usable from 12 to 44MHz.

Surface defect characterization: Figures 17 and 18, respectively, show the indications of finely scribed indentations on the surfaces of glass plate and a dense BeO substrate. It should be mentioned here that in order to appreciate the observations of surface irregularities by the utilization of surface wave device, this phenomenon is best visualized while the transducer is scanned on the defects, such as by surface acoustic microscopy or other similar mechanisms. For example, the surface crack in BeO substrate identified in Fig. 18 is clearly shown by an image generated by advanced C-scanning, Fig. 19. The crack is estimated to be $5\mu\text{m}$ deep in BeO.

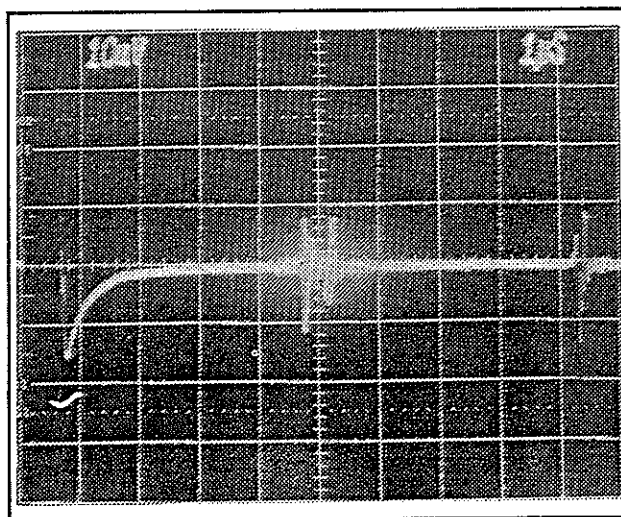


Fig. 15. Entire realtime rf trace of a 25MHz, 6mm, 1 na GA transducer on a glass plate. Central HIGHLIGHTED region: 1st reflection, longitudinal wave directly reflected from glass surface in water. 2nd reflection, surface wave in glass plate.

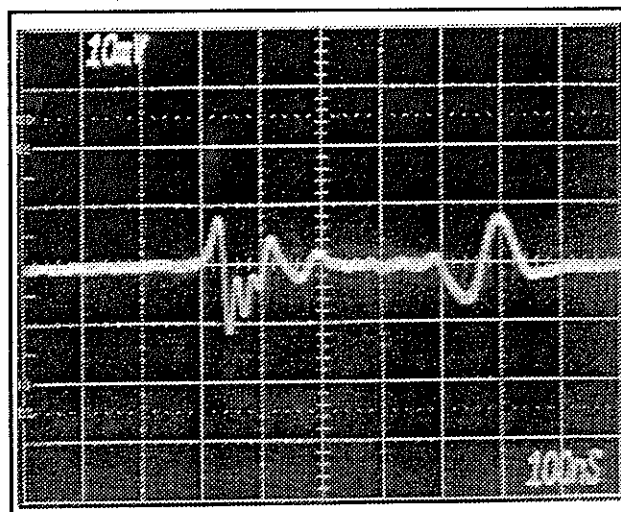


Fig. 16. Same as Fig. 14, except the central HIGHLIGHTED region has been amplified from $1\mu\text{s/d}$ to 100ns/d . LEFT: Longitudinal wave RIGHT: Surface wave.

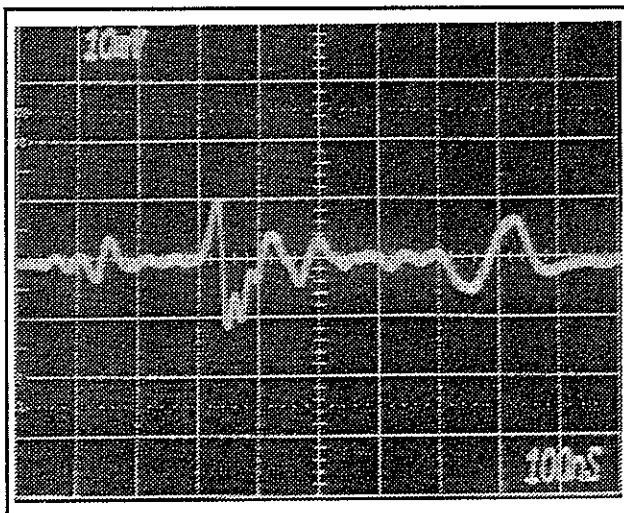


Fig. 17. Indication of surface-breaking crack on a glass plate.

LEFT: Appearance of the surface crack, $\sim 50\mu\text{m}$.

MIDDLE: Longitudinal wave

RIGHT: Surface wave in glass.

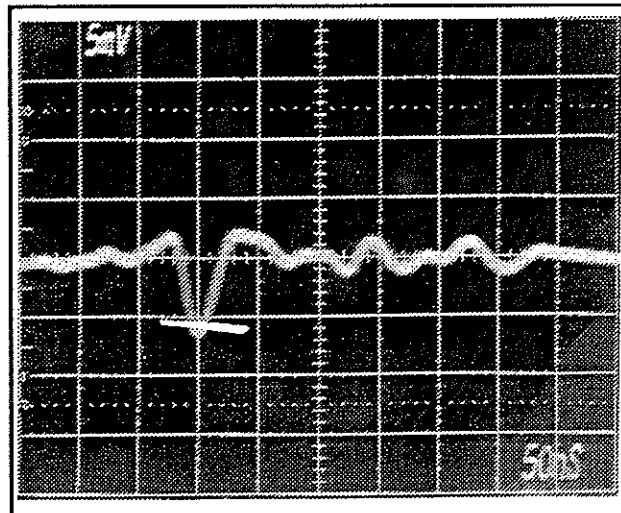


Fig. 18. Indication of surface-breaking crack on a BeO substrate.

LEFT: Longitudinal wave

MIDDLE: Surface crack, $\sim 5\mu\text{m}$.

RIGHT: Surface wave in BeO.

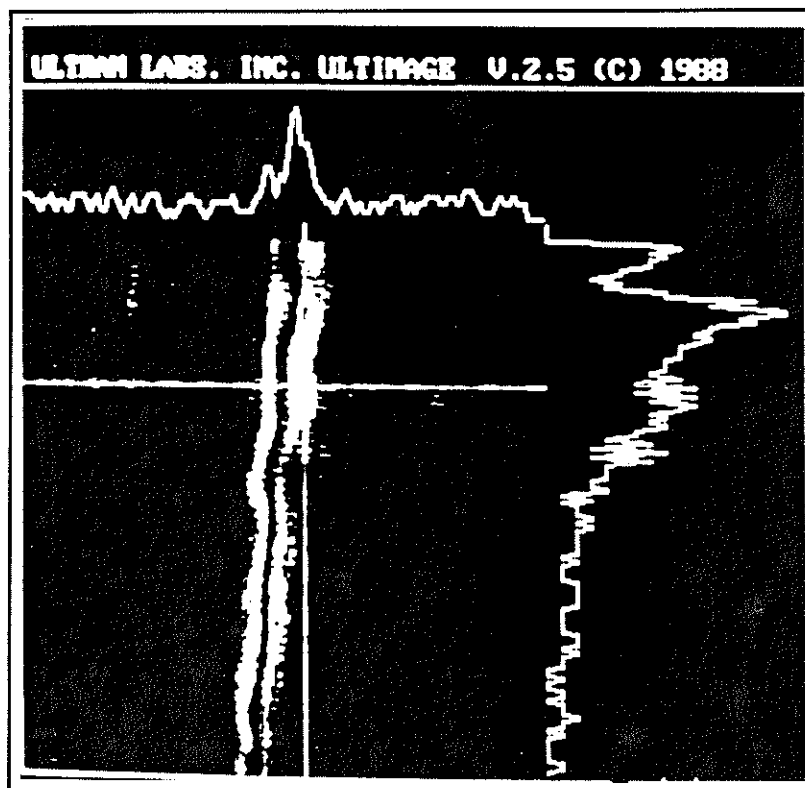


Fig. 19. An ultrasonic image of $\sim 5\mu\text{m}$ surface crack in dense BeO produced by scanning a 25MHz, 1.0na GA transducer on the sample in water. Top and right hand cross-sectional profiles indicate the intensity of ultrasound as a function of transducer location on and around the cracked region. This information can be applied to estimate the severity of damage relative to the material composition and microstructure.

Styles of GEOMETRICAL ACOUSTICS transducers

Although we have only described the applications of immersion type GA transducers, similar devices for their direct contact applications have also been produced in our laboratory.

CONCLUSIONS

In this paper we have presented significant developments into critical transducer technology from our laboratory. Novel, yet simple transducer designs described here facilitate a variety of NDC applications, which would have been otherwise impossible. Value of these advancements in ultrasonics will undoubtedly enhance the cause of materials quality and reliability through nondestructive characterization.

ACKNOWLEDGEMENTS

The work presented in this publication has been supported by the on-going ultrasonic projects - targeted at establishing new standards of NDC for the advancement of materials quality and reliability.

REFERENCES

1. Bhardwaj, M.C., "Ultrasonic NDC - A Historical Perspective and Practical Concepts," a publication of Ultrason Laboratories, Inc., Series on NDC, EPN-101a, July 1987.
2. Brunk, J., "Applications of Dry Contact Ultrasonic Transducers," Proceedings, 11th World Conference, NDT, ASNT, v. 2 (1985).
3. Brunk, J., "An Investigation of Dry Contact Ultrasonic Gauging," a report prepared for US DOE, Contract # De-AC04-76-DP00613, avail. NTIS (1986).
4. Brunk, J., "Performance Comparison of Dry Coupling Contact Ultrasonic Transducers, 0.5 to 20MHz," proceedings, NDE Symp., SWRI, San Antonio, TX, (1987).
5. Bhardwaj, M.C., "Importance and Use of Very High Frequency Ultrasound in Nondestructive Characterization of Materials," *Cer. Bull.*, v. 65, no. 11, (1986).
6. Ultrason Laboratories, Inc., "Lambda Transducers: Their Features and Applications in Nondestructive Characterization of Materials," a publication of Ultrason Laboratories, Inc., Series on NDC, EPN-104, (1982).
7. Gilmore, R., Tam, K.C., and Howard, D.R., "Acoustic Microscope from 10 to 100MHz for Industrial Applications," GE Corporate R&D Tech. Report: 86RDC015 (1986).
8. Bergmann, L., "Der Ultraschall und seine Anwendung in Wissenschaft und Technik," Ultrasonics and Their Applications in Science and Technology, S. Hirzel Verlag, Zurich (1954).